J. Min. Metall. Sect. B-Metall. 53 (1) B (2017) 61 - 66

Journal of Mining and Metallurgy, Section B: Metallurgy

ENHANCED ELECTROCHEMICAL PERFORMANCES OF $LiNi_{0.5}Mn_{1.5}O_4$ BY SURFACE MODIFICATION WITH Cu NANOPARTICLES

G. Zhao[a,b], Y. Lin[a,b,*], W. Zhu[a,b], W, Yang[a,b], Z. Huang[a,b,#]

[a] Fujian Provincial Key Laboratory of Quantum Manipulation and New Energy Materials, College of Physics and Energy, Fujian Normal University, Fuzhou, China

[b] Fujian Provincial Collaborative Innovation Center for Optoelectronic Semiconductors and Efficient Devices, Xiamen, China

(Received 06 September 2015; accepted 12 July 2016)

Abstract

5V spinel $LiNi_{0.5}Mn_{1.5}O_4$ cathode is prepared by traditional solid-state method and nano-Cu particles were derived from a chemical reduction process. The effect of Cu-coating on the electrochemical performances of $LiNi_{0.5}Mn_{1.5}O_4$ cells, in a wide operation temperature range (-10℃, 25℃, 60℃), is investigated systematically by the charge/discharge testing, cyclic voltammograms and impedance spectroscopy, respectively. The results demonstrate that the modified material exhibits remarkably enhanced electrochemical reversibility and stability. Cu-coated material has much lower surface and charge-transfer resistances and shows a higher lithium diffusion rate. The Cu coating layer as a highly efficient lithium ion conductor, acted as a highly efficient protector to restrain the contact loss.

***Keywords**: Lithium-ion battery; Cathode; Surface modification; $LiNi_{0.5}Mn_{1.5}O_4$*

1. Introduction

Mastering energy storage and conversion has become primordial under the great pressure of environment and energy crisis with the ongoing global warming and the depletion of crude oil. Li-ion battery bas been extensively studied for hybrid electric vehicle (HEV) and plug-in hybrid electric vehicle (PHEV) application due to their high favorite properties of lightness, compactness, working voltage and energy densities compared to other technologies for the past two decades [1-4]. To keep up with the large application of 3G techniques to cell phones and the fast development of laptop central processing, high-energy and high-power density are required. Numerous effects have been paid to search new materials with high energy density as the capacity of commercialized cathode materials (e.g. $LiCoO_2$) is limited [5]. Among the studied cathode materials, $LiNi_{0.5}Mn_{1.5}O_4$ cathode material is one of the most promising candidates for large size Li-ion batteries because of its specific capacity of about 140mAhg^{-1} and a higher voltage (4.7 V) [6-8] .

The $LiNi_{0.5}Mn_{1.5}O_4$ cathode can be assembled into high-energy density-type full cells and coupled with a high power-type anode to assemble power-type full cells [9-10]. However, the instability of the cell has become the best barrier impeding of the commercialization of $LiNi_{0.5}Mn_{1.5}O_4$ cathodes. That is, at such a high charge/discharge potential, the normal $LiPF_6$-based alkyl carbonate electrolyte decomposes via various mechanisms upon long term cycling, which ultimately leads to the rapid electrode dissolution by hydrogen fluoride attack and polarization due to a formation of surface film. All of these mechanisms are even more accelerated at elevated temperatures [11-17].

For this purpose, a simple chemical reduction process is employed to deposit the uniform distribution of nano-sized Cu particles on the surface of $LiNi_{0.5}Mn_{1.5}O_4$ composites to provide a highly conductive nanolayer between particles and protects the active materials from chemical attack by HF in electrolyte. The as-prepared $LiNi_{0.5}Mn_{1.5}O_4$-Cu exhibits superior electrochemical performances in a wide operation temperature range compared to the pristine $LiNi_{0.5}Mn_{1.5}O_4$.

2. Experimental

2.1 Preparation and characterization of cathode materials

The pure $LiNi_{0.5}Mn_{1.5}O_4$ cathode material was prepared through traditional solid-state method,

Corresponding author: yblin@fjnu.edu.cn, zghuang@fjnu.edu.cn#*

DOI:10.2298/JMMB150906021Z

respectively. Appropriate amounts of $LiOH•H_2O$, $Ni(NO_3)_3$ and electrolytic MnO_2 were mixed in a ball-milling machine with anhydrous ethanol as dispersant for 2 h. Then the chemical mixture is preheated at 600 ℃ for 5h followed by milling for another 12h. Subsequently, the precursor was sintered at 800 ℃ for 15h to obtain final products.

For coating Cu on $LiNi_{0.5}Mn_{1.5}O_4$ cathode material, $CuCl_2$ in the stoichiometric ration were dissolved in absolute ethanol, the as-prepared $LiNi_{0.5}Mn_{1.5}O_4$ powder was added into the above absolute ethanol and ultrasonically dispersed for 1h. And then the sodium borohydride ($NaBH_4$) solution in a molar ratio of 5:2 to $CuCl_2$ dissolved in absolute ethanol ether were added drop by drop into the continuously agitated solution. The reactant suspensions were kept by stirring at room temperature, washed 3 times with absolute ethanol, and subsequently dried at 70 ℃ in vacuum to get the final product.

2.2 Cell fabrication and characterization

The electrochemical properties were measured on the test standard R2025 coin cells. The cathode electrodes for the electrochemical evaluation were prepared by homogeneously coating a slurry containing 80 wt.% active material, 10 wt.% super-P and 10 wt.% polyvinylidene fluoride (PVDF) dissolved in N-methyl-2-pyrrolidone onto an aluminum foil and dried in vacuum for 12 h at 120 ℃. Assembled Standard R2025 coin cells in an Ar-filled glove box(O_2 < 3ppm and H_2O < 3ppm) (Mikrouna, Super 1220/750), using lithium metal foil as anode electrode, Celgard 2300 microporous polyethylene membrane as the separator and 1M solution of $LiPF_6$ in a 1:1:1 (by volume) mixture of dimethyl carbonate (DMC), ethylene carbonate (EC) and ethyl methyl carbonate (EMC) as electrolyte. Cells were charged and discharged versus Li^+/Li on a battery cycle (LAND, CT2001A).

2.3 Characterization of cathode materials

The morphologies and distributions of the prepared powders were observed using scanning electron microscopy (SEM, JSM-7500F). The phase identification of the pristine $LiNi_{0.5}Mn_{1.5}O_4$ and Cu coated $LiNi_{0.5}Mn_{1.5}O_4$ powders was conducted with an X-ray diffractometer (XRD, Rigaku MiniFlex II) using CuKa radiation (λ=0.154056 nm), X-ray profiles were measured between 10° and 80° (2θ angle) with a scan step of 0.02° and a scan speed of $8°min^{-1}$.

The charge–discharge performance of the test cell was applied with LAND 2001A apparatus. Cyclic voltammetry (CV) was developed at a series scan rate on an electrochemical workstation (CHI, 650B). Electrochemical impedance spectroscopy (EIS) was recorded with applied 5 mV sinusoidal perturbation in a frequency range from 10 mHz to 100 KHz at room temperature .The spectra were analyzed by Z-view software.

3. Results and discussion

Typical XRD patterns of $LiNi_{0.5}Mn_{1.5}O_4$ and ($LiNi_{0.5}Mn_{1.5}O_4$) /Cu denoted as Samples A and B, are shown in Fig.1 (a), respectively. Two sets of XRD patterns can be indexed well based on a cubic spinel structure (ICSD#070046). The spinel $LiNi_{0.5}Mn_{1.5}O_4$ is not affected after coating powder with Cu within the sensitivity of measurement. The finding of no evidence of diffraction peaks corresponding to Cu was expected since the low quantity .This can be confirmed by the analysis of elemental EDS results. The analysis of the surface layer for EDS $LiNi_{0.5}Mn_{1.5}O_4$/Cu is present in Fig. 1(b). Analysis of EDS results confirm the presence of Cu on the $LiNi_{0.5}Mn_{1.5}O_4$ and the corresponding content of Cu is approximately estimated as 2 wt. %.

Fig.2 shows the morphologies of Samples A and B. A smooth and clean surface was observed on the $LiNi_{0.5}Mn_{1.5}O_4$ particles (Fig. 2a). The surface smooth and clean was changed after Cu treat. As Cu nanoparticles with ~20 nm were found to be uniformly distributed over the surface of $LiNi_{0.5}Mn_{1.5}O_4$ particles in Fig. 2b, The Cu can form a conducting network to provide pathways for electron transfer between particles.

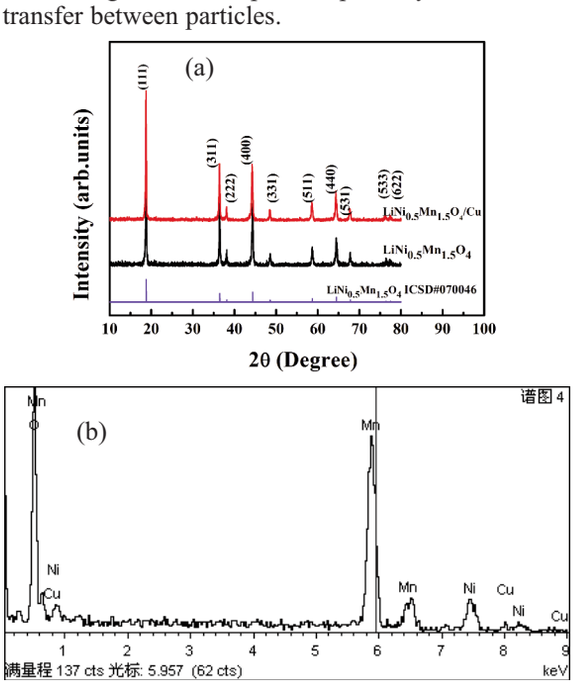

Figure 1. *(a) XRD patterns of Samples A and B, (b) the EDS of the $LiNi_{0.5}Mn_{1.5}O_4$/Cu composite*

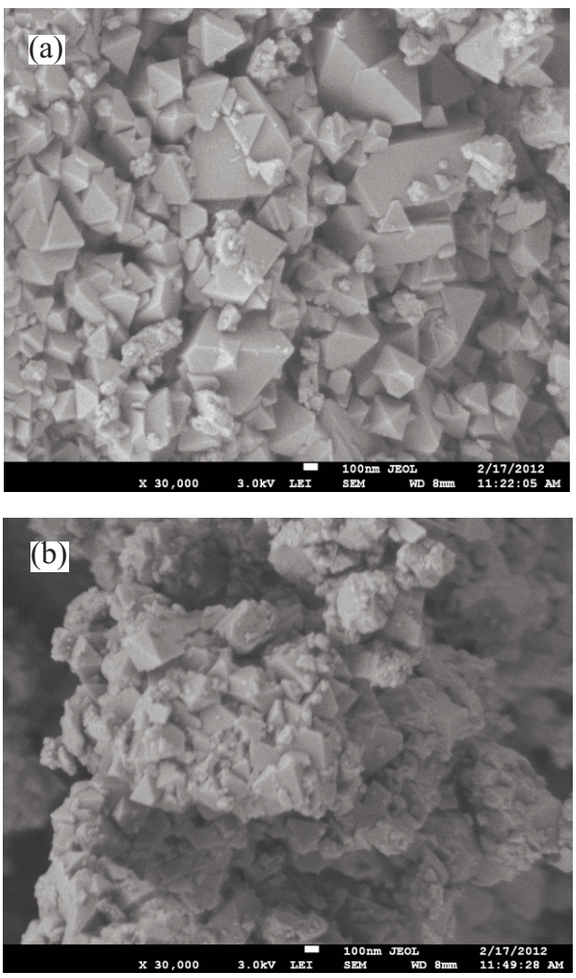

Figure 2. *SEM photographs of (a) the as-prepared $LiNi_{0.5}Mn_{1.5}O_4$ and (b) $LiNi_{0.5}Mn_{1.5}O_4$/Cu material*

Fig. 3(a) shows the typical cycle life curves of the electrodes comprising Samples A and B between 3.0 and 4.9 V at 25 ℃, for the pristine $LiNi_{0.5}Mn_{1.5}O_4$. From the Fig. 3(a), it is found that the discharge capacity decrease from ~119 to 66 $mAhg^{-1}$ after 100 cycles at 2C, and only 56 % of capacity retained. In contrast, Cu-coated $LiNi_{0.5}Mn_{1.5}O_4$ still delivers a capacity of 101 $mAhg^{-1}$ with capacity retention of 93.8 % after 100 cycles, which means that Cu coating clearly improves the cycle stability of $LiNi_{0.5}Mn_{1.5}O_4$. The reduced polarization and better discharge performances of the $LiNi_{0.5}Mn_{1.5}O_4$/Cu are ascribed to the conduct coating layer protected the surface of the active materials from HF.

To examine the effectiveness of Cu coating on improving the rate capacity of the cathode material, the specific capacities at different discharge rates are investigated and showed in Fig. 3(b). The Cu-coated $LiNi_{0.5}Mn_{1.5}O_4$ electrode exhibits enhanced rate capability obviously compared with the $LiNi_{0.5}Mn_{1.5}O_4$. When the discharge rate increase from 0.2C to 4C, the capacity retention of Samples A and B are 59 % and 84 %, respectively. It is speculated that the Cu coating layer stabilizes the structure of cathode materials at higher current density, and acts as highly efficient lithium ion conductor.

Cyclic votammogram (CV) tests were conducted to better understand the electrochemical behavior of the pristine and coated $LiNi_{0.5}Mn_{1.5}O_4$. Figs. 4(a)-(d) show the CV curves at sweep rates of 0.03, 0.05, 0.08 and 0.1 mV s^{-1} ranging from 3.0 to 4.9 V, respectively. The major doublet redox peaks at around 4.7 V and 4.8 V originate from the Ni^{+2}/Ni^{+3} and Ni^{+3}/Ni^{+4} redox couple, and the small doublet redox peak in 4.0 is ascribed to the Mn^{+3}/Mn^{+4} redox. As shown in Figs. 4(c) and (d), the peak current (i_p) has a square root dependence on the sweep rate ($v^{1/2}$). The apparent diffusion coefficient can be derived according to following Eq. [18-20]:

$$I_p = 2.69*10^5 n^{3/2} A D^{1/2} C_{Li} v^{1/2} \quad (1)$$

Where I_p is the peak current, n is the number of charge-transfer involved in the reaction, A is the contact area of the electrode and electrolyte (cm^2), C_{Li} is the lithium ions concentrations in the cathode (mol cm^{-3}) and v is the scan rate (Vs^{-1}). The difference in Li^+ diffusion coefficients (D) is the reflection of difference in the rate of transport for lithium ions in the electrodes. The results indicate that the diffusion coefficient of Li^+ cause by Mn^{3+}/Mn^{4+}, Ni^{2+}/Ni^{3+}, Ni^{3+}/Ni^{4+} transition are calculated as $5.66*10^{-11}cm^2s^{-1}$,

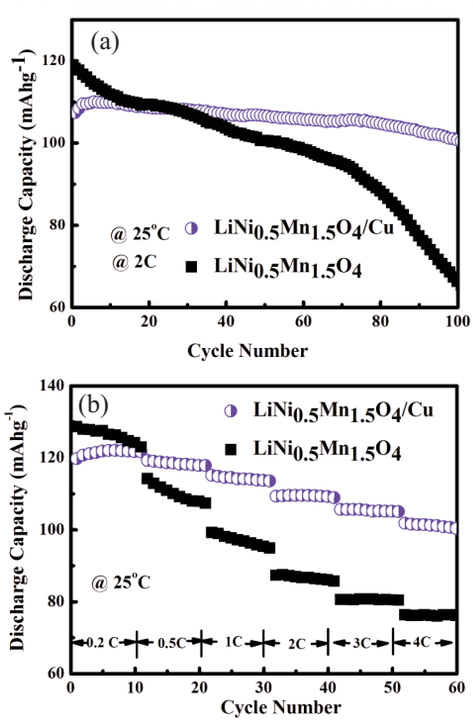

Figure 3. *(a) Cycling behavior at 2C and (b) Rate capabilities of Samples A and B at 25℃*

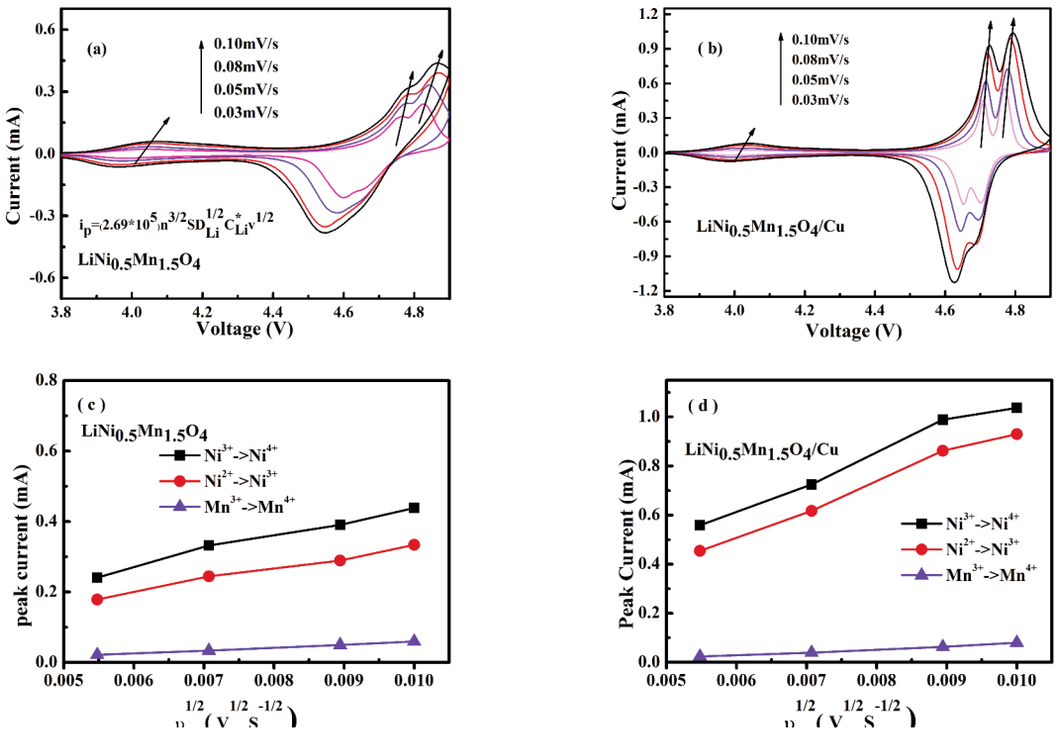

Figure 4. *(a, b) CV curves at a series of sweep rates and (c, d) relationship between the peak current and the square root of sweep rate for Sample A and B*

$3.7*10^{-11}$ cm^2s^{-1}, $1.11*10^{-10}$ cm^2s^{-1} for Sample A and $8.41*10^{-11}$ cm^2s^{-1}, $1.23*10^{-10}$ cm^2s^{-1}, $2.94*10^{-10}$ cm^2s^{-1} for Sample B .The data clearly demonstrate that the kinetics of Li^+ diffusion is be enhanced by coating high electronic conductivity Cu on $LiNi_{0.5}Mn_{1.5}O_4$ surface due to the enhancement in electronic conductivity, resulting in the superior rate behavior [21].

Fig. 5(a) illustrates the cycling performances of the samples A and B in the voltage range of 3-4.9 V in 2C at 60 ºC. From the Fig. 5(a), it is found that the capacity of sample A decreases quickly and remaining only 37.5 % of the initial capacity after 100 cycles. However, the decrease of the capacity for the coated sample is substantially alleviated, and a capacity retention of 80 % is obtained (The initial capacity of 118.6 $mAhg^{-1}$ is decreased to 95 $mAhg^{-1}$ after 100 cycles).This outstanding stability of the coated sample should result from the more stable spinel structure during charge-discharge process. This cycling behavior of the Cu-coated electrode material shows clearly the impact of Cu coating in protecting the surface of $LiNi_{0.5}Mn_{1.5}O_4$ against HF attack [11]. At the same time, the sample B exhibits greatly improved long-cycle life and relatively high rate performance, as shown in Fig 5b. The discharge capacity of the sample B decreases less than that of the sample A. It is speculated that the Cu-coated acts as a highly efficient protector to restrain the contact loss in the interface of the electrode/current collector and the

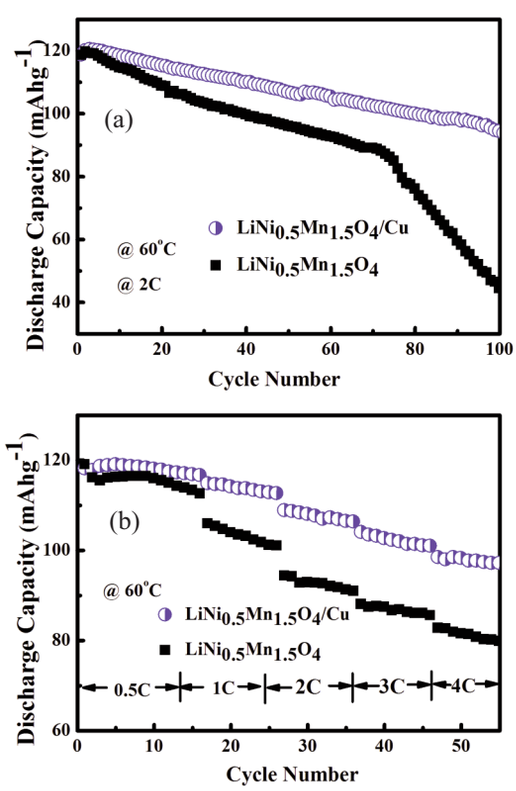

Figure 5. *(a) Cycling behavior at 2C and (b) Rate capabilities of pristine and Cu-coated $LiNi_{0.5}Mn_{1.5}O_4$ at 60 ℃*

interface between the $LiNi_{0.5}Mn_{1.5}O_4$ particles. Such contact loss will lead to capacity fading. The contact loss inside the electrode layer generates some isolated $LiNi_{0.5}Mn_{1.5}O_4$ particles that are no more active for charge and discharge reaction [14].

To understand the electrochemical dynamic behavior of electrodes, electrochemical impedance spectroscopy (EIS) measurements are performed using the cells after 90 cycles at 2C and 60 ºC. As shown in Fig. 6a, the semicircle in the high-frequency region represents the resistance of Li^+ ion migration through the surface layer, and another semicircle in the medium-to-low frequency range is attributed to the charge transfer resistance. Moreover, the sloping line at low frequency region is ascribed to the diffusion of Li^+ in the solid electrode [22]. The equivalent electrical circuit model shown in Fig.6b is used to analyze impedance spectra. The impedance spectra can be explained with electrolyte resistance (R_e), charge-transfer resistance (R_{ct}), Warburg impedance (Z_w), surface resistance (R_s), nonideal capacitance of the surface layer (CPEs), and nonideal capacitance of the double layer (CPE_{dl}) [21,23]. According to the equivalent circuit, individual contribution from each of solution resistance, diffusion resistance and charge-transfer resistance are calculated as 55.96 Ω, 129.1 Ω and 156.8 Ω for Sample A and 36.33 Ω, 70.45 Ω and 62.96 Ω for Sample B, respectively. R_{ct} of the sample B is much smaller than that of the sample A, and the increase of electronic conductivity greatly reduces the charge transfer resistance. As the byproducts generated in the electrolyte decomposition process are able to adhere on the surface of the positive electrode,which is highly resistive to Li ion transport, covering the electrode surface would delay the Li^+ kinetics [24-26].

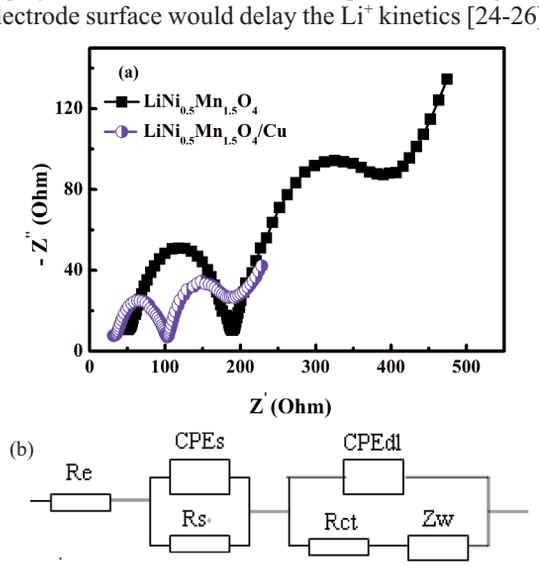

Figure 6. *(a) The EIS profiles of $LiNi_{0.5}Mn_{1.5}O_4$ and Cu-coated $LiNi_{0.5}Mn_{1.5}O_4$ at the fully discharge state and the equivalent circuit (b)*

Partial surface degradation of the active material by the HF gives rise to an increase in interfacial resistance, so that the pristine $LiNi_{0.5}Mn_{1.5}O_4$ demonstrated larger contact and charge transfer resistances and a poor rate capability [27].

Fig.7 presents the discharge capacity of the electrodes at different C rates at -10 ºC. As the C rate increased, the Cu-coated samples exhibited a noticeably higher discharge capacity. The stable Cu-coating layer could suppress the formation of unwanted interface layer and protect the cathode from the reactive electrolyte, which facilitates the rapid movement of electrons and Li ions during the charge-discharge process.

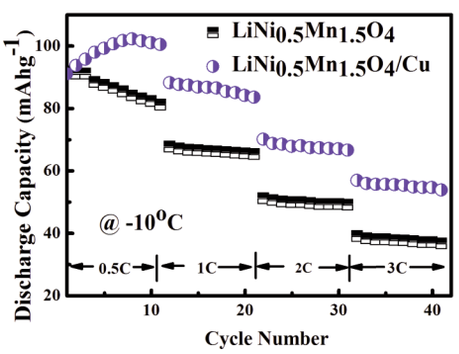

Figure 7. *Rate capabilities of pristine and Cu-coated $LiNi_{0.5}Mn_{1.5}O_4$ at -10 ℃*

4. Conclusions

Nano-sized Cu particles were successfully deposited on the surfaces of $LiNi_{0.5}Mn_{1.5}O_4$ particles by a simple chemical reduction process. Compared to the pristine $LiNi_{0.5}Mn_{1.5}O_4$, Cu-coating $LiNi_{0.5}Mn_{1.5}O_4$ exhibits superior electrochemical performances in a wide operation temperature range. The presence of Cu-coating-layer on $LiNi_{0.5}Mn_{1.5}O_4$ surface is considered to play a positive role in decreasing the interfacial impedance, enhancing lithium diffusion rate and suppressing the dissolution of active materials in the LiPF6 based electrolyte.

Acknowledgement

We acknowledge the financial support by National Fundamental Research Program of China (No. 2011CBA00200), the Natural Science Foundations of China (No. 11344008, 11204038), Science and Technology Major Projects of Fujian Province (2013HZ0003), Project of Fujian Development and Reform Commission (2013-577), and Project of Fujian Province Educational Department (JA15119).

References

[1] S.Monao, F. De Giorgio, L. Da Col, M. Riché, C. Arbizzani, M. Mastragostino, J. Power Sources, 278 (2015) 733-740.

[2] J.S. Chae, M.R.Jo, Y. Kim, J. Ind. and Eng. Chem, 21 (2015)731-735.

[3] G. B. Zhong, Y. Y. Wang, Z. C. Zhang, C. H. Chen. J. Electrochim. Acta, 56 (2011) 6554-6561.

[4] D. Liu, J. Trottlier, P. Charest, J. Frechette, A. Guerfi, A. Mauger, C. M . Julien, K. Zaghib, J. Power Sources 204 (2012)127-132.

[5] J.G. Yang, X.L. Zhang, Z.Q. Zhu, J. Electroanal. Chem, 688 (2013) 113-117.

[6] X. Fang, Y. Lu, N. Ding, X.Y. Feng, C. Liu, C.H. Chen, J. Electrochim. Acta, 55 (2010) 832-837.

[7] L.P. Wang, H.Li, X.J Huang, E. Baudrin, J.Solid State Ionics,193 (2011) 32-38

[8] G.B. Zhong, Y.Y. Wang, Y.Q. Yu, C.H. Chen, J. Power Sources 205 (2012) 385-393.

[9] J. Mao, K.H. Dai, Y.C. Zhai, J. Electrochim. Acta 63 (2012) 381-391.

[10] S. Brutti, V. Gentili, P. Reale, L. Carbone, S. Panero, J. Power Sources 196 (2011) 9792-9799.

[11] Y.K. Sun, K.J. Hong, J. Prakash, K. Amine, J. Electrochem. Commun. 4 (2002) 344-348.

[12] R. Kostecki, F. McLarnon, Electrochem. J. Solid State Lett. 7 (2004) A380-A383.

[13] Y. Talyosef, B. Markovsky, G. Salitra, D. Aurbach, H.J. Kim, S. Choi, J. Power Sources 146 (2005) 664-669.

[14] T. Yoon, S.J. Park, J.Y. Mun, J.H. Ryu, W. Choi , Y.S. Kang ,J.H. Park, M. Seung M, J. Power Sourse 215 (2012) 312-316.

[15] S.T. Myung, Y. Hitoshi, Y.K. Sun, J. Mater. Chem. 21 (2011) 9891-9911.

[16] B. Markovsky, Y. Talyossef, G. Salitra, D. Aurbach, H. Kim, S. Choi, J. Electrochem. Commun. 6 (2004) 821-826.

[17] D. Aurbach, B. Markovsky, Y. Talyossef, G. Salitra, H. J. Kim, S. Choi, J. Power Sources 162 (2006) 780-789.

[18] Y. Jin, C.P. Yang, X.H. Rui, T. Cheng, C.H. Chen, J. Power Sources 196 (2011) 5623-5630.

[19] X.H. Rui, N. Ding, J. Liu, C. Li, C.H. Chen, J. Electrochim. Acta 55 (2010) 2384-2390.

[20] X. Fang, N. Ding, X.Y. Feng, Y. Lu, C.H. Chen, J. Electrochim. Acta 54 (2009) 7471-7475.

[21] T.Y. Yang, N.Q. Zhang, Y. Lang, K.N. Sun, J. Electrochim. Acta 56 (2011) 4058-4064.

[22] J. Liu, A. Manthiram, J. Electrochem. Soc.156 (2009) A833- A 838.

[23] J. Liu, A. Manthiram, J. Chem. Mater.21 (2009)1695-1707.

[24] D. Aurbach, J. Power Sources 119-121 (2003)497-503.

[25] S.T. Myung, K. Izumi, S. Komaba, Y.K. Sun, H. Yashiro, N. Kumagai, J. Chem. Mater. 17 (2005) 3695-3704.

[26] S.T. Myung, K. Izumi, S. Komaba, H. Yashiro, H.J. Bang, Y.K. Sun, N. Kumagai, J. Phys. Chem. 111 (2007) 4061-4067.

[27] H.B. Kang, S.T. Myung, K. Amine, S.M. Lee, Y.K. Sun, J. Power Sources 195 (2010) 2023-2028.